Molecular Basis for Differential Nucleotide Binding of the Nucleotide-Binding Domain of ABC-Transporter CvaB†

Xiangxue Guo,‡ Xianfeng Chen,‡ Irene T. Weber,§ Robert W. Harrison,|| and Phang C. Tai*,‡

Department of Biology, Department of Chemistry, and Department of Computer Science, Georgia State University, Atlanta, Georgia 30303

Received July 26, 2006; Revised Manuscript Received September 28, 2006

ABSTRACT: The cytoplasmic membrane protein CvaB, involved in colicin V secretion in *Escherichia coli*, belongs to the ABC-transporter family in which ATP hydrolysis is typically the driving force for substrate transport. However, our previous studies indicated that the nucleotide-binding domain of CvaB could also bind and hydrolyze GTP and, indeed, highly preferred GTP over ATP at low temperatures. In this study, we have examined the molecular basis of this preference. Sequence alignment and homology modeling of the CvaB nucleotide-binding domain predicted that the aromatic stacking region of CvaB (Y^{501}DSQ loop) had a role in the differential binding of nucleotides, and Ser^{503} and Gln^{504} provided potential hydrogen bonds to GTP but not to ATP. Site-directed mutagenesis of the Y^{501}DSQ loop, mutations S503A, Q504L, and double mutation S503A/Q504L, was made to test the predicted hydrogen bonds with GTP. The double mutation S503A/Q504L increased the affinity for ATP by 6-fold, whereas the affinity for GTP was reduced slightly: the ATP/GTP-binding ratio increased about 10-fold. The temperature effect assays on nucleotide binding and hydrolysis further indicated that the double mutant protein had largely eliminated the difference for substrates ATP and GTP, and behaved more similarly to the NBD of typical ABC-transporter HlyB. Therefore, we conclude that Ser^{503} and Gln^{504} in aromatic stacking region of CvaB block the ATP binding and are important for the GTP-binding preference.

Colicin V (ColV),[1] an antibacterial toxin produced by *Enterobacteriaciae*, kills sensitive target cells by disrupting their cell membrane potential (*1*). In the Gram-negative bacterium *Escherichia coli*, ColV is secreted by a dedicated type I exporter system across both the cytoplamic and outer membranes directly into the environment outside the cells. At least three protein components participate in the ColV export system: two plasmid-borne proteins CvaA and CvaB in the cytoplasmic membrane and a host chromosomal gene product TolC in the outer membrane (*2*, *3*).

The cytoplasmic membrane protein CvaB plays pivotal roles in the ColV export system. CvaB belongs to the family of ATP-binding cassette transporters (*4*, *5*), like the α-hemolysin exporter HlyB (*6*), the cystic fibrosis transmembrane conductance regulator (*7*), and the multidrug resistance P-glycoprotein (*8*). The N-terminal proteolytic domain of CvaB processes the leader region of the ColV precursor at the double glycine site (*9*−*11*), the transmembrane domains in the middle of CvaB form the cytoplasmic channel (*3*, *9*, *12*), and the C-terminal nucleotide-binding domain supplies energy for ColV secretion. Although the sequence of the proteolytic N-terminal domain of CvaB is unique among ABC transporters (*11*), the C-terminal nucleotide-binding domain (NBD) retains a high level of homology with other family members (*4*, *5*, *13*). Several highly conserved ABC-NBD motifs are found in the CvaB sequence, such as the Walker A and B sites, the ABC Signature motif, the Q-loop, and the H-switch (*14*−*17*). The Walker A and B sites are common to most ATPases involved in the binding and hydrolysis of nucleotides, while the ABC Signature motif is highly specific to ABC-NBDs. The Q-loop and H-switch are also specific to ABC transporters; they interact with the bound magnesium nucleotide through noncovalent forces, such as ionic or hydrogen bond interactions (*16*). Three main aspects of nucleotide binding are noted by analysis of crystal structures of bacterial ABC-NBDs, such as HlyB (*6*), HisP (*18*), MJ0796 (*19*), MalK (*20*, *21*), and GlcV (*22*). First, the Walker A and B sites interact with oxygen atoms on the β- and γ-phosphates of bound nucleotide and orientate the nucleotide phosphates in the protein nucleotide-binding pocket (*17*). Second, the nucleotide-binding cofactor magnesium (Mg^{2+}) is important for connecting the nucleotide and protein through the ionic and hydrogen bond interactions involving oxygen atoms from β- and γ-phosphates of the nucleotide and from residues of the Walker A and B sites and the Q-loop directly or via a water molecule (*22*). The magnesium stabilizes the nucleotide in the binding site and participates directly in the nucleotide hydrolysis (*17*). Third, amino acid residues from the ABC Signature motif are also

† This work was supported in part by National Institutes of Health Research Grants GM34766 (P.C.T.) and GM65762 (R.W.H.), Georgia Cancer Coalition (R.W.H. and I.T.W.), and Molecular Basis of Disease Program Fellowship (X.G.), Georgia Research Alliance and Research Enhancement Program from Georgia State University.

* To whom correspondence should be addressed: phone, 404-651-3109; fax, 404-651-2509; e-mail, biopct@langate.gsu.edu.

‡ Department of Biology, Georgia State University.

§ Department of Chemistry, Georgia State University.

|| Department of Computer Science, Georgia State University.

[1] Abbreviations: ABC, ATP-binding cassette; ColV, colicin V; NBD, nucleotide-binding domain; NTP, nucleotide triphosphate; PDB, Protein Data Bank.

10.1021/bi061506i CCC: $33.50
Published on Web 11/09/2006

involved in the binding of nucleotide as shown in the ABC-NBD dimer structures (*19*, *20*, *23*, *24*).

Alignment of the sequences of bacterial ABC transporters revealed that CvaB-NBD is phylogenetically the most similar to the HlyB-NBD. HlyB is a typical ATP-binding cassette protein on the cytoplasmic membrane that acts in the export of α-hemolysin in *E. coli* (*6*). Although the HlyB lacks the proteolytic domain at the N-terminus for processing substrate precursor that is present in CvaB (*11*), their C-terminal NBDs share a high sequence similarity. Recent studies indicated that the HlyB-NBD functions as a dimer providing energy for substrate transport (*24*, *25*), while the nucleotide-dependent formation of the CvaB-NBD dimer has also been reported (*26*). In an active ABC transporter, ATP hydrolysis is widely assumed to supply energy (*14*−*16*, *27*, *28*) for the translocation process. Many crystal structures of the ABC-NBD are stabilized by binding ADP or ATP analogues (*6*, *29*, *30*), and site-directed mutagenesis of the conserved binding sites will affect the binding and hydrolysis of nucleotide (*31*). Biochemical studies indicated that the bound ATP interacted extensively with the HlyB-NBD nucleotide-binding sites (*6*, *24*), induced the dimerization of the protein (*26*, *32*), and showed cooperation in the ATP hydrolysis (*25*). However, our previous results in vitro indicated that the CvaB-NBD had highly preferential binding of GTP at low temperatures, and the hydrolysis of ATP is cold-sensitive compared to that of GTP (*33*). In this study, we have determined the molecular basis of the nucleotide-binding preference of CvaB-NBD. Homology modeling of the CvaB-NBD dimer identified potential interacting residues for differential binding of nucleotides, and site-directed mutagenesis of those residues was used to test the binding and hydrolysis of nucleotides at different temperatures. The results showed that the aromatic loop (Y^{501}DSQ) is involved in the high GTP-binding preference of CvaB.

MATERIALS AND METHODS

Bacterial Strains, Plasmids, Media, and Reagents. E. coli strains DH5α [K12 *supE44* Δ*lacU169* (*ϕ*80 *lacZ*ΔM15) *hsdR17 recA1 endA1 gyrA*96 *thi-1 relA1*] (*34*) and BL21 (B F^- *ompT* $hsdS_B$) (*35*) were used as the hosts for plasmid transformation and protein expression, respectively. Plasmid pHK11 contains genes *cvaA*, *cvaB*, *cvaC*, and *cvaI* (*36*). Plasmid pPSG122 (a gift from Dr. Schmitt) expresses the N-terminal His-tagged fusion protein HlyB-NBD (residues 467−707) under the control of an arabinose-inducible promotor in pBAD18 (*6*). The vector pTrcHisB is used for expressing CvaB-NBD (residues 459−698) (Invitrogen Corp., Carlsbad, CA).

Bacterial culture medium TA (10 g of tryptone and 5 g of NaCl per liter with buffer A: 40 mM potassium phosphate buffer (pH 7.0) with 7.6 mM ammonium sulfate and 1.6 mM sodium citrate) was used as both the liquid and solid plates (with 1.5% agar). The antibiotics ampicillin and chloramphenicol were used at a final concentration of 100 and 30 μg/mL, respectively. Restriction enzymes, T4 DNA ligase, and EDTA-free protease inhibitor were obtained from Roche Applied Sciences Inc. (Indianapolis, IN) and were used essentially as recommended by the manufacturer. All other chemicals were of reagent grade and were purchased from Sigma Corp. (St. Louis, MO) unless otherwise noted.

Construction, Expression, and Purification of CvaB-NBD. Recombinant DNA manipulations were performed essentially as described (*37*). Wild type and mutants of CvaB-NBD with the His_6 tag on the N-terminus were expressed with the vector pTrcHisB. For high-level expression, the constructed plasmid was freshly transformed into the host *E. coli* BL21, and the overnight cell culture was diluted 40 times into fresh TA medium and cultivated at 37 °C until the OD_{600} was between 0.4 and 0.6; then the culture was induced by 0.5 mM isopropyl β-D-thiogalactopyranoside (IPTG) at 27.5 °C for 4 h. CvaB-NBDs were purified from cell supernatant through Ni-NTA (Qiagen Inc., Valencia, CA) affinity, Q-Sepharose FF ion exchange, and Superose 6 FPLC (Pharmacia Corp., Peapack, NJ) gel filtration chromatography. The purified proteins were stored at −80 °C in 100 mM 3-(cyclohexylamino)propanesulfonic acid (CAPS) buffer (pH 10.4) with 20% glycerol and 10 mM DTT.

Construction of CvaB-NBD Models with Nucleotides. The molecular model of CvaB-NBD was built by homology to the templates of the HlyB-NBD monomer [PDB entry 1MT0 (*6*)] and dimer [PDB entry 1XEF (*24*)] crystal structures, respectively. The molecular modeling program AMMP was used as described (*38*, *39*). The HlyB-NBD dimer structure provided the ATP and Mg as templates to generate the ATP- and GTP-bound models of CvaB-NBD. The ligand structure (Mg and ADP) of TAP1-NBD (PDB entry 1JJ7) (*29*) was also considered when docking nucleotides onto CvaB-NBD. A discrete water model was used to treat solvation. The new atoms in the hydrated dimer models were generated by 20 cycles of the analytic procedure of AMMP (*38*) with molecular mechanics potentials. Finally, the models were optimized by 1000 steps of conjugate gradient minimization.

Site-Directed Mutagenesis. Plasmid DNA isolation, digestion, transformation, and other routine DNA manipulations were as described (*37*). Mutagenesis was performed by overlap extension PCR with pHK11 as the template (*40*). DNA sequencing was performed to verify the mutations, using an ABI 377 sequencer (Applied Biosystems, Forster City, CA) in the Biology Core Facilities, Georgia State University.

Gel Electrophoresis, Western Blotting, and Western Blot. Standard SDS−polyacrylamide gel electrophoresis was performed according to the method of Laemmli (*41*). For Western blotting, electrophoresed proteins were transferred to poly(vinylidene difluoride) membranes (Applied Biosystems, Foster City, CA) and treated by established procedures for Western blotting (*42*). The polyclonal antibody for CvaB-NBD was made using the 12 kDa C-terminus of CvaB (*33*). Alkaline phosphatase-conjugated goat anti-rabbit IgG (Bio-Rad Laboratories, Hercules, CA) was used as the secondary antibody.

ATP/GTP UV Cross-Linking and Competitive Binding. UV cross-linking was performed as described (*43*). Samples (20 μL) containing 2 μg of CvaB-CTD protein and 1 μM α-^{33}P-labeled ATP or GTP (3000 Ci/mmol from Perkin-Elmer Inc., Boston, MA) were preincubated for 5 min on ice in the binding buffer (20 mM Tris-HCl, pH 8.0, 100 mM NaCl, 5 mM $MgCl_2$). Samples were irradiated in an XL-1000 UV cross-linker (Spectronics Inc., Westbury, NY) at 254 nm at 120 mJ/cm^2 twice for 15 min in an ice−water bath or twice for 10 min at other temperatures (16, 25, and 37 °C) as indicated. Cross-linked samples were directly mixed in SDS

loading buffer and separated by 12% SDS−PAGE. The gel was dried, and the radioactive bands were quantified by a PhosphorImager (Fujifilm Medicals, Edison, NJ).

For the competitive binding assay, after the proteins were incubated with radioactive nucleotides, different concentrations of nonradioactive ATP or GTP were added to compete on ice for 10 min, and then UV irradiation was performed as described (*44*). The competitive binding data were fitted to the linear regression by Prism (GraphPad Software Inc., Ober-Olm, Germany) to obtain the best fit and half of the effective concentration, which were displayed as R^2 and EC_{50}, respectively.

ATPase/GTPase Activity Assay. The complete reaction mixture (20 μL) contained 5 mM magnesium chloride, 100 mM potassium acetate, 40 mM Tris−acetate (pH 7.5), 2 μg of ovalbumin, 1 mM DTT, and 0.5 μg of CvaB-NBD protein. [γ-^{33}P]GTP or [γ-^{33}P]ATP (1 μCi; Perkin-Elmer Inc., Boston, MA) was added to samples incubated at various temperatures. The assay was carried out as described (*33*). Briefly, after 10 min incubation at the temperatures indicated, the reaction mixtures were mixed with 800 μL of a 5% suspension of activated charcoal (Sigma Corp., St. Louis, MO) in 20 mM phosphoric acid, incubated on ice for 10 min, and then centrifuged for 10 min to pellet the charcoal and absorbed nucleotides. A 200 μL aliquot of the supernatant fraction containing the liberated radioactive phosphate was analyzed by a Beckman scintillation counter. Sample data were normalized by subtracting the background count from the control without CvaB-NBD protein.

The temperature effect on NTPase activities was calculated according to the Arrhenius equation ($k = Ae^{-E_a/RT}$). Here, k is the reaction rate constant at different temperatures, R is equal to 0.00831 kJ mol^{-1} K^{-1}, E_a is the activation energy (kJ/mol), T is temperature (K), and A is the frequency factor as ln(k) intercept. The slopes ($-E_a/R$) of the ln(k) vs 1/T linear relationship displayed the activation energy of the reaction (E_a) at different temperatures.

RESULTS

Differential Binding of Nucleotides by HlyB and CvaB. Our previous studies have shown that the CvaB-NBD (C-terminal domain of CvaB, residues 459−698) binds GTP with much higher affinity than ATP at low temperatures (*33*). In this work, further analysis of this preference for binding GTP was made in comparison with that of the typical ABC-transporter HlyB nucleotide-binding domain (HlyB-NBD). As reported previously (*33*), the GTP-binding level of CvaB-NBD was about 12.5 times higher than that for binding ATP shown on their nucleotide-bound amount. Similar binding trends were observed when using radioactive ADP and GDP (data not shown). In contrast, the HlyB-NBD cross-linked nucleotides with a slight preference for ATP compared with GTP (Figure 1). The results suggested that CvaB may be unique among ABC transporters in the preference for binding GTP.

In order to determine the molecular basis of the nucleotide-binding preference, the sequences of CvaB and other ABC transporters were aligned. The sequences shared similar Walker A and B sites, ABC Signature motif, D-loop, Q-loop, and H-switch regions (Figure 2). High identity (42.9%) and similarity (61%) were especially evident for the NBDs of

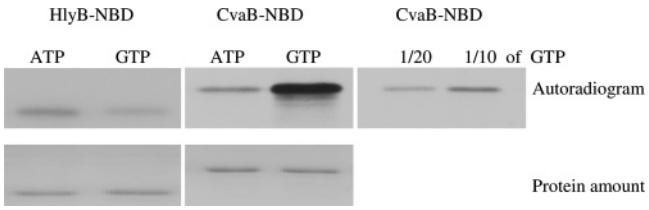

FIGURE 1: Different nucleotide-binding preferences of CvaB-NBD and HlyB-NBD at 0 °C. The protein amount was indicated by Coomassie blue staining (below). The radioactive GTP-bound CvaB-NBD was diluted 10 and 20 times for comparison with the ATP-bound form.

HlyB and CvaB. Analyzing ABC-NBD sequences and available crystal structures suggested some residues provided hydrogen bonds and hydrophobic interactions with the base ring of bound nucleotides. Conserved aromatic residues (Tyr or Trp) were identified recently to stack on the nucleotide base ring in the multidrug resistance protein (*15*, *45*). The corresponding aromatic stacking region of CvaB is the Y^{501}DSQ loop (Figure 2). Since the ATP and GTP molecules differ only in their purine rings, the Y^{501}DSQ-loop region was proposed to be responsible for the differential nucleotide binding of CvaB-NBD.

Modeling CvaB-NBD Interactions with Nucleotides. To further investigate the interactions of CvaB-NBD with the bound nucleotides, molecular models were built of the structure of CvaB-NBD in complex with ATP or GTP. In the models, the Walker A and B sites interacted very similarly with the magnesium and β- and γ-phosphates of the two nucleotides, ATP or GTP. The CvaB-NBD dimer model predicted that the Signature motif was also involved in the binding of β- and γ-phosphates of nucleotide but showed no significant differences in the interaction with ATP or GTP (data not shown).

Analysis of the molecular models predicted a stacking interaction between the aromatic rings of the conserved Tyr^{501} and the nucleotides GTP or ATP. This stacking interaction was a little weaker for ATP than for GTP considering the separation of the aromatic groups of 4.2 and 3.9 Å, respectively (Figure 3). Furthermore, Ser^{503} and Gln^{504} of the Y^{501}DSQ loop formed two hydrogen bonds to the guanine base of GTP, Ser^{503}-O$\gamma\cdots$N^2-GTP and Gln^{504}-O$\epsilon^1\cdots$N^2-GTP (Figure 3, right), which are not possible for ATP due to the lack of an N^2 group on the purine ring. No equivalent interaction appears in the model of CvaB-NBD with bound ATP (Figure 3, left). These potential hydrogen bonds were predicted to increase the binding affinity for GTP compared to ATP. Therefore, the molecular models support our previous observation (*33*) that CvaB-NBD bound preferentially to GTP over ATP. Instead of the classical nucleotide-binding sites (Walker A and B and the Signature motif), the Y^{501}DSQ loop was predicted to be important for the preferential binding of CvaB-NBD to GTP rather than ATP.

Lack of Effect on GTP Preference for Residues of the Walker A Site, B Site, or ABC Signature Motif. Site-directed mutagenesis experiments were designed to test the predictions of homology modeling. Comparing the NBD sequences of CvaB and HlyB, several variable residues were found in the Walker A and B sites. Ala^{527}, Ala^{530}, and Thr^{533} (A site) and Phe^{652} and Met^{653} (B site) of CvaB differed from the consensus sequence (Table 1).

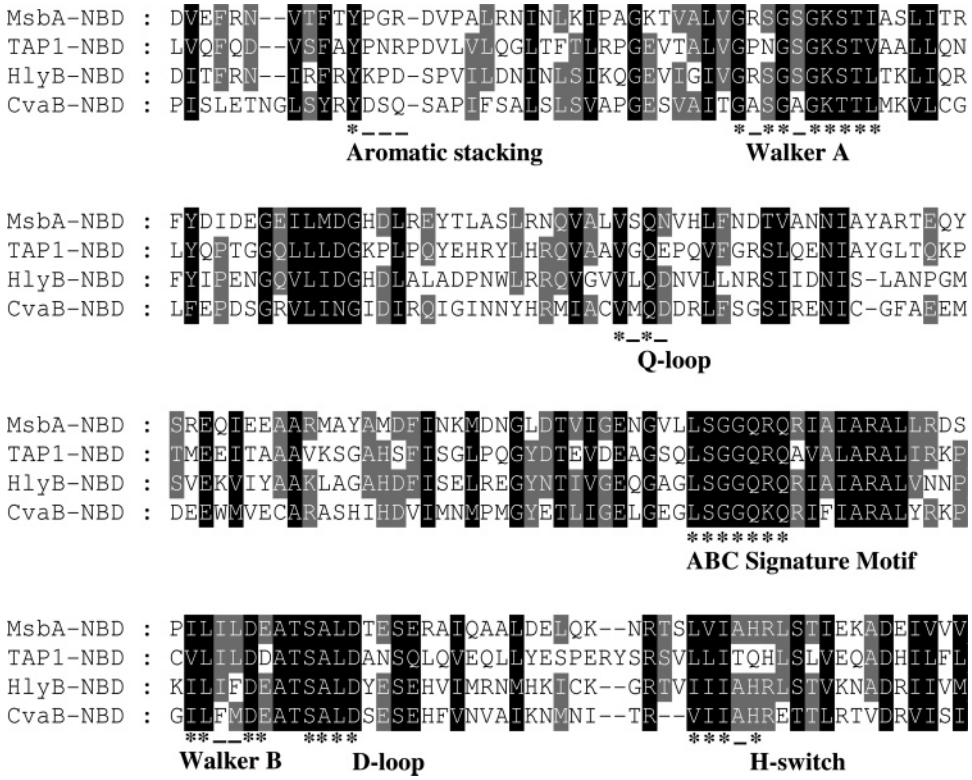

FIGURE 2: Alignment of the NBD sequences of CvaB and other ABC transporters. All NBD protein sequences are from *E. coli* except the TAP1-NBD, which is an endoplasmic reticulum resident protein in *Homo sapiens*. (HlyB, transporter for α-hemolysin; TAP, transporter associated with the antigen process; MsbA, transporter for lipid A.) [Note: (1) the gray and dark colors show the conservation of amino acid residues of the protein sequence; (2) identical or nearly identical residues in each conserved site are marked by an asterisk.]

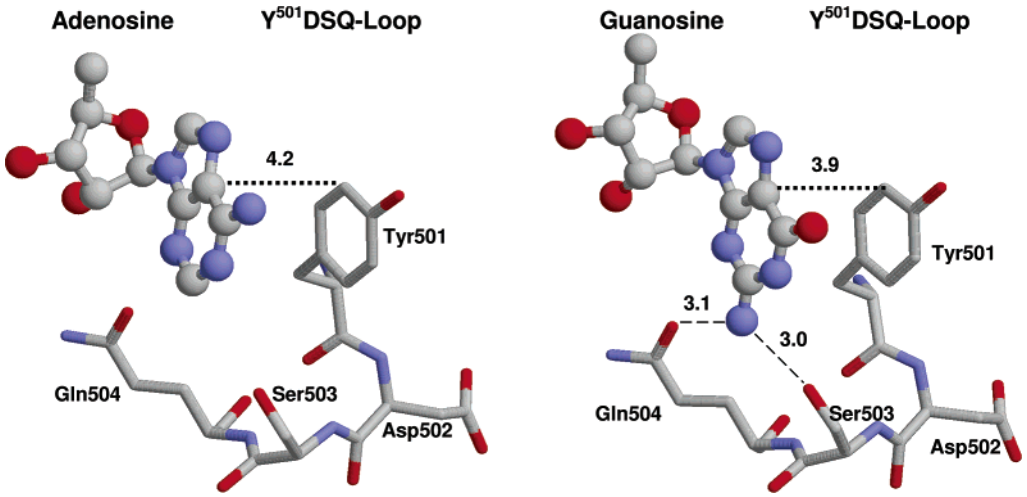

FIGURE 3: Predicted interactions between the side chains of the Y^{501}DSQ loop and the bases of the bound nucleotide ATP (left) and GTP (right). The molecular model was illustrated with the molecular visualization software RasMol (http://www.umass.edu/microbio/rasmol/); the color red indicates oxygen, gray is carbon, and blue is nitrogen atoms. Dashed lines indicate hydrogen bonds, and dotted lines are stacking interactions, with interatomic distances in Å. A distance cutoff of 3.2 Å was used to identify hydrogen bonds.

Site-directed mutagenesis of those variable residues in the Walker A and B sites was performed to test the effect on differential binding of ATP or GTP to CvaB. Mutant proteins with the single-site substitutions (A527R, A530S, T533S, F652I, and M653F) and their combinations were purified and tested by UV cross-linking to radioactive ATP or GTP. Only the double mutation A527R/A530S on the Walker A site decreased the GTP/ATP-binding ratio by about 25%, and this decrease was partially recovered if this double mutation was combined with the double mutation F652I/M653F on the Walker B site (Table 1). Single mutations and other double or triple mutations did not show much difference in the ratio of GTP or ATP binding. These results showed that phylogenetically variable residues in the Walker A and B sites did not account for the high GTP-binding preference of CvaB-NBD, as predicted.

Site-directed mutagenesis of the ABC Signature motif of CvaB showed similar results for the UV cross-linking to ATP and GTP. While the G633D and K635A mutants showed similar ATP- and GTP-binding levels to those of wild type, the mutant Q634H showed significantly reduced levels for binding of both GTP and ATP. However, the GTP/ATP-binding ratio was similar to that of wild type (Table 1). These results demonstrated that, like the Walker A and B sites, the

Table 1: Site-Directed Mutagenesis on Walker A and B Sites and the Signature Motif of CvaB-NBD[a]

	Walker A	Walker B
CvaB	G-**A**^{527}-S-G-**A**^{530}-G-K-**T**^{533}-T……I-L-**F**^{652}-**M**^{653}-D-E	
HlyB	G-**R**^{503} -S-G-**S**^{506}-G-K- **S**^{509} -T……I-L-**I**^{628} -**F**^{629} -D-E	
Consensus	G-**R** -S-G-**S** -G-K -**S** -T……I-L -**I** -**L** -D-E	

mutants	location	G/A ratio
wild type	wild type	12.5 ± 0.7
A527R	Walker A	10.2 ± 0.5
A527R-A530S	Walker A	8.9 ± 0.5
T533S	Walker A	13.0 ± 0.5
A527R-T533S	Walker A	12.7 ± 0.9
F652I	Walker B	11.9 ± 0.5
M653F	Walker B	12.9 ± 0.7
M653L	Walker B	12.1 ± 0.5
F652I-M653F	Walker B	11.4 ± 0.9
F652I-M653L	Walker B	11.7 ± 0.6
A527R-F652I-M653F	Walker A and B	10.0 ± 0.5
A527R-T530S-F652I-M653F	Walker A and B	9.4 ± 0.9
G633D	Signature motif	12.1 ± 0.5
Q634H	Signature motif	9.1 ± 0.3
K635A	Signature motif	13.5 ± 0.4

[a] The G/A ratio is the average value of the nucleotide-bound amount of three repeats.

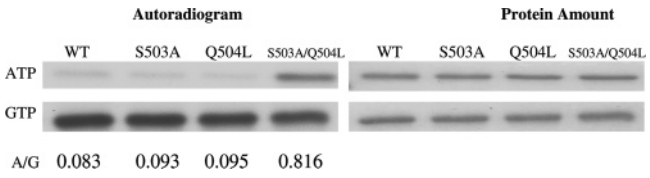

FIGURE 4: The double mutation in the Y^{501}DSQ loop changes the preference of CvaB-NBD for binding GTP at 0 °C. (A/G: the ratio of the binding amount for ATP and GTP normalized by protein amounts.)

ABC Signature motif was not involved in differential binding of ATP and GTP.

ATP-Binding Enhancement in the Double Mutant of the Y^{501}DSQ Loop. To test if the aromatic stacking region (residues 501−504) was indeed involved in the differential binding of nucleotides ATP and GTP as predicted, the single mutations S503A and Q504L and the double mutant S503A/Q504L were made. The substitutions of serine to alanine and glutamine to leucine replaced their polar side chains with hydrophobic side chains of approximately similar size. Purified wild-type and mutant proteins were tested by UV cross-linking to [α-^{33}P]ATP and [α-^{33}P]GTP, respectively. The autoradiogram results indicated that the single-mutation proteins S503A and Q504L had little effect on the ATP/GTP-binding ratio. However, the double mutant protein S503A/Q504L showed about 6-fold increase in binding affinity for ATP while that of GTP was reduced slightly, compared with those of the wild-type protein. The ATP/GTP-binding ratio of mutant S503A/Q504L increased from 0.08 to 0.8, about 10 times more than that of the wild type (Figure 4). Thus, the double mutant protein S503A/Q504L largely eliminated the high preference of wild-type CvaB-NBD for GTP by increasing the affinity for ATP at low temperatures.

Reduced Preference for GTP of the Double Mutant Protein S503A/Q504L. To further analyze the affinity for different nucleotides by the double mutant protein S503A/Q504L, the binding of radioactive [α-^{33}P]ATP or [α-^{33}P]GTP to CvaB-NBDs was competed by a series of concentrations of cold ATP or GTP. Their half effective concentrations (EC_{50}) were

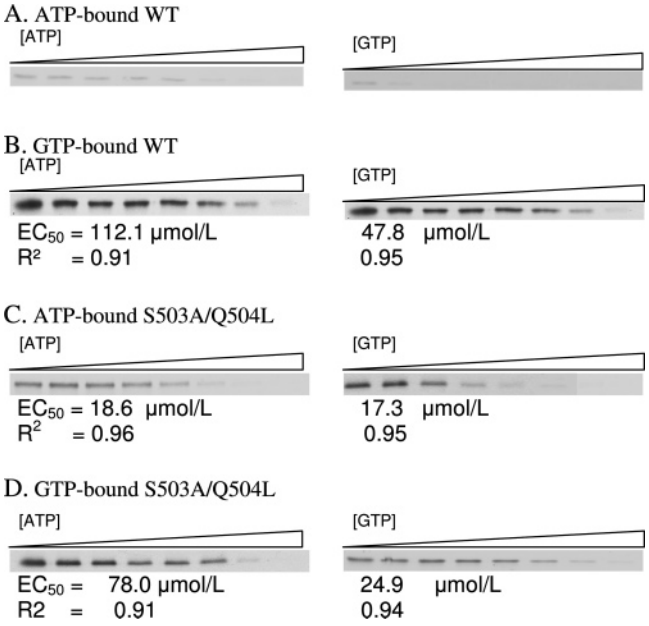

FIGURE 5: Competitive binding assay of wild-type CvaB-NBD and the mutant. Radiolabeled nucleotides (at 0 °C) bound to CvaB-NBD or the mutant protein were competed at 0 °C by cold ATP and GTP, respectively. Concentrations of cold ATP or GTP were 0, 6.25, 12.5, 25, 50, 100, 250, and 500 μmol/L, from left to right. All samples were exposed for 3 h in (A) ATP-bound WT, (B) GTP-bound WT, (C) ATP-bound S503A/Q504L, and (D) GTP-bound S503A/Q504L.

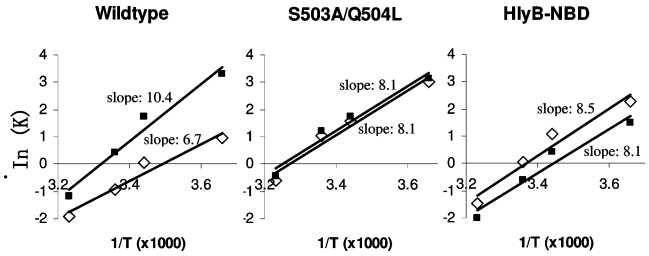

FIGURE 6: Temperature sensitivity of the binding affinity for ATP (◇) and GTP (■). Data used were average values of three repeats.

calculated as an estimate of the nucleotide-binding affinity. For the radioactive GTP-bound wild type, the EC_{50} of cold ATP was as high as 112.1 μM while that of GTP was 47.8 μM (Figure 5B), indicating the high GTP affinity for CvaB-NBD wild type. Data for ATP-bound wild-type protein (Figure 5A) were not shown due to the low ATP-binding level, which resulted in inaccurate scanning.

However, the double mutant protein S503A/Q504L showed different competition patterns for the ATP-bound and GTP-bound forms. Nonradioactive ATP and GTP displayed a similar low competitive level (Figure 5C) for the radioactive ATP-bound double mutant protein. However, for the radioactive GTP-bound double mutant protein, more than 3-fold of nonradioactive ATP was needed compared with that of GTP (Figure 5D). It appeared that the double mutant protein S503A/Q504L still slightly preferred GTP over ATP, though the degree of preference was much lower than that of the wild type.

Temperature Effects of the Double Mutant on Binding of Nucleotides and ATP/GTPase Activity. The temperature effects of the double mutant on the binding of nucleotides were assayed by UV cross-linking. As reported previously (*33*), the UV cross-linking of GTP or ATP by CvaB-NBD

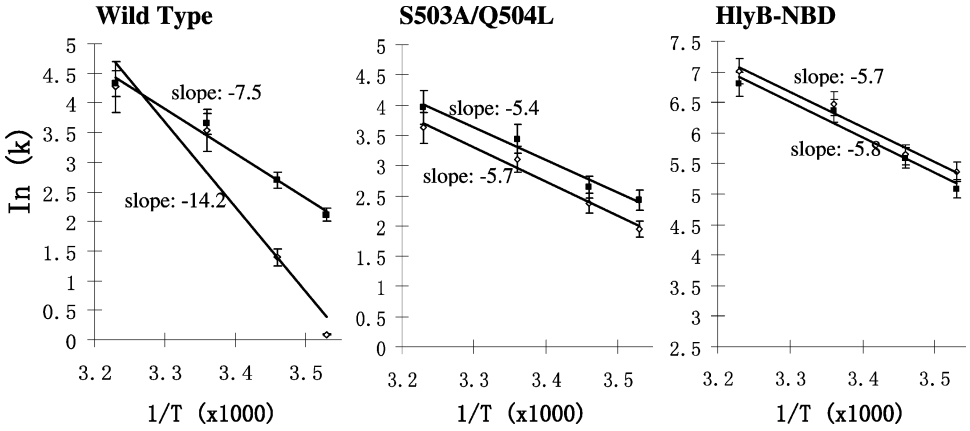

FIGURE 7: Temperature sensitivity of hydrolysis activity for ATPase (◇) and GTPase (■). The temperature effects were calculated on the basis of the Arrenhius equation; data used were average values of three repeats.

decreased with the increase of temperatures, likely due to molecular motion. However, in contrast to the wild type, the double mutant protein displayed relatively similar binding levels for ATP and GTP at different temperatures (Figure 6).

At the same time, the ATP/GTPase activities of the double mutant protein were further tested at different temperatures. As reported previously (*33*), the ATPase activity in the wild-type CvaB was cold-sensitive: the ATPase activity became 8−10 times lower than that of GTPase at 10 °C. However, for the double mutant protein S503A/Q504L, the ATPase activity at low temperatures increased to a level similar to that of the GTPase activity (Figure 7).

From those temperature effect assays, it was concluded that the double mutant protein changed the properties of the wild type on both the nucleotide binding and hydrolysis and behaved more closely to HlyB-NBD, which is a typical ABC transporter.

DISCUSSION

In bacterial cells, the physiological concentration of ATP is about 10 times higher than that of GTP, and it is widely assumed that the ATP hydrolysis supplies energy to an active ABC-translocation process (*14*−*16*, *27*, *28*). However, our results showed the GTP-binding preference of CvaB-NBD at lower temperatures in vitro. This is different from most of the NBDs of a typical ABC transporter, such as HlyB (*25*, *27*) and MalK (*21*), although the potential meaning of physiological function is not clear. In this study, we examined the molecular basis of the differential binding of CvaB-NBD to ATP and GTP at low temperatures. The approaches utilized were modeling of the CvaB-NBD bound to different nucleotides to search for potential interactions and then site-directed mutagenesis to verify those predictions. Mutations of the traditional nucleotide-binding motifs, such as the Walker A and B sites and the ABC Signature motif, had little effect on the preference of CvaB-NBD for GTP over ATP (Table 1). On the other hand, the recently identified aromatic stacking region in the Y^{501}DSQ loop of CvaB-NBD was predicted to provide two potential hydrogen bonds to GTP but not to ATP (Figure 3). Amino acid substitutions were designed to remove the two potential hydrogen bonds. Thus, the hydrophilic side chains of Ser^{503} and Gln^{504} were replaced by the hydrophobic side chains of alanine and leucine, respectively, which cannot form hydrogen bonds. Site-directed mutagenesis results indicated that, unlike the wild-type CvaB-NBD, the double mutant protein S503A/Q504L increased both the binding affinity for ATP (Figure 4 and 6) and the ATPase activities to almost same level as for GTP at low temperatures (Figure 7). We conclude that the Y^{501}DSQ loop directly participated in the differential binding of nucleotides and the double mutant S503A/Q504L largely eliminated the high GTP preference of CvaB-NBD at low temperatures by increasing the binding affinity for ATP.

It is worth noting that the double mutant did not decrease the GTP binding significantly (only about 30% of GTP-binding decrease was observed in Figure 4), which is not as huge a difference as we expected. Hence, we consider the Ser^{503} and Gln^{504} function to block ATP from binding to the NBD of CvaB, and the replacement of those two residues largely increases the ATP binding at the lower temperatures. However, the GTP binding of the double mutant is quite intense, compared to NBDs of HlyB and other ABC transporters. Due to the complexity of the enzyme−substrate interaction, we suspect that other factors, such as the angle between aromatic rings of Tyr^{501} and nucleotide, may also contribute to the GTP-binding preference of CvaB-NBD, which needs to be further studied.

The aromatic stacking effect has been observed in some crystal structures of ABC transporters, such as human TAP1 (*29*), MalK (*21*), and MJ0796 (*46*), and described by Locher (*14*), Schmitt (*15*), and Higgins (*16*). Site-directed mutagenesis and biochemical studies of the aromatic residue of HisP (*47*) and MRP1 (multidrug resistance protein) (*45*) showed the significance of the aromatic ring for the binding of nucleotide. In this study, we provide evidence for specific interactions between residues of the Y^{501}DSQ loop and the base ring of different nucleotides using both homology modeling predictions and site-directed mutagenesis and suggested the mechanism of the highly preferential binding of CvaB-NBD to GTP. Two hydrogen bonds were predicted between the side chains of Ser^{503} and Gln^{504} and the N^2 group of GTP, which cannot occur in ATP due to lack of the 2-amino group on the purine ring. The absence of these potential hydrogen bonds may produce little difference in stacking observed in the model between aromatic rings of Tyr^{501} and the ATP.

The aromatic stacking loop has been found in many ABC transporters. However, only the aromatic residue (Y or F) is

conserved (*45*, *48*, *49*); the other residues are very variable (Figure 2). Possibly, it is the unique subdomain structure of the CvaB YDSQ loop that differentiates between the base rings of nucleotides ATP and GTP. The replacement of amino acids in the HlyB aromatic region (Y^{477}KPD), substituting serine for proline and glutamine for aspartic acid, did not change the trends in ATP/GTP binding of HlyB-NBD (data not shown). Recently, the dimeric crystal structure of HlyB-NBD was obtained in complex with nucleotide (*24*). Through docking with different nucleotides in the crystal structure, it was found that the corresponding aromatic stacking region of HlyB-NBD did not display any significant preference for nucleotides. Possibly the reason is that Pro^{479} and Pro^{482} made a sharp turn in the structure of the aromatic region (Y^{477}KPDSPVIL), which might prevent the residues, such as Asp^{480} and Ser^{481}, from interacting with the GTP base. Thus, the HlyB-NBD was predicted to show similar affinity for both ATP and GTP, consistent with our experimental results, which identified a slight preference for binding ATP (Figure 1). The temperature effects of HlyB-NBD on nucleotide binding and hydrolysis were also characterized (Figures 6 and 7) in comparison with the effects on the wild type and double mutant of CvaB-NBD. The double mutant S503A/Q504L behaved similarly to HlyB-NBD, indicating that the double mutation of the aromatic stacking region (Y^{501}DSQ loop) had changed the GTP preference of CvaB-NBD. We conclude that sequence and structural differences in the aromatic stacking region are important for the specific nucleotide preference of NBDs.

ACKNOWLEDGMENT

We thank Dr. L. Schmitt at the Institute of Biochemistry, Goethe University, Frankfurt, Germany, for providing the HlyB-NBD expression plasmid pPSG122 and the reviewers for constructive comments. We also thank Dr. Bing Na and Ms. Jiali Zhou at the Department of Biology, Georgia State University, for making some of the site-directed mutations.

REFERENCES

1. Zhang, L. H., Fath, M. J., Mahanty, H. K., Tai, P. C., and Kolter, R. (1995) Genetic analysis of the colicin V secretion pathway, *Genetics 141*, 25−32.
2. Fath, M. J., Skvirsky, R. C., and Kolter, R. (1991) Functional complementation between bacterial MDR-like export systems: Colicin V, alpha-hemolysin, and Erwinia protease, *J. Bacteriol. 173*, 7549−7556.
3. Gilson, L., Mahanty, H. K., and Kolter, R. (1990) Genetic analysis of an MDR-like export system: The secretion of colicin V, *EMBO J. 9*, 3875−3894.
4. Ames, G. F. L., Mimura, C. S., Holbrook, S. R., and Shyamala, V. (1992) Traffic ATPases: A superfamily of transport proteins operating from *Escherichia coli* to humans, *Adv. Enzymol. 65*, 1−47.
5. Higgins, C. F. (1992) ABC transporters: from microorganisms to man, *Annu. Rev. Cell Biol. 8*, 67−113.
6. Schmitt, L., Benabdelhak, H., Blight, M. A., Holland, I. B., and Syubbs, M. T. (2003) Crystal structure of the nucleotide binding domain of the ABC-transporter haemolysin B: Identification of a variable region within ABC helical domains, *J. Mol. Biol. 330*, 333−342.
7. Vergani, P., Lockless, S. W., Nairn, A. C., and Gadsby, D. C. (2005) CFTR channel opening by ATP-driven tight dimerization of its nucleotide-binding domains, *Nature 433*, 876−880.
8. Altenberg, G. A. (2004) Structure of multidrug-resistance proteins of the ATP-binding cassette (ABC) superfamily, *Curr. Med. Chem.: Anti-Cancer Agents 4*, 53−62.
9. Fath, M. J., Skvirsky, R. C., and Kolter, R. (1994) Purification and characterization of colicin V from *Escherichia coli* culture supernatants, *Biochemistry 33*, 6911−6917.
10. Hävarstein, L. S., Holo, H., and Nes, I. F. (1994) The leader peptide of colicin V shares consensus sequences with leader peptides that are common among peptide bacteriocins produced by gram-positive bacteria, *Microbiol. 140*, 2383−2389.
11. Zhong, X., Kolter, R., and Tai, P. C. (1996) Processing of colicin V-1, a secretable marker protein of a bacterial ATP binding cassette export system, requires membrane integrity, energy, and cytosolic factors, *J. Biol. Chem. 271*, 28057−28063.
12. Kerr, I. D. (2002) Structure and association of ATP-binding cassette transporter nucleotide-binding domains, *Biochim. Biophys. Acta 85536*, 1−18.
13. Fath, M. J., and Kolter, R. (1993) ABC transporters: Bacterial exporters, *Microbiol. Rev. 57*, 995−1017.
14. Locher, K. P. (2004) Structure and mechanism of ABC transporters, *Curr. Opin. Struct. Biol. 14*, 426−431.
15. Schmitt, L., and Tampé, R. (2002) Structure and mechanism of ABC transporters, *Curr. Opin. Struct. Biol. 12*, 754−760.
16. Higgins, C. F., and Linton, K. J. (2004) The ATP switch model for ABC transporters, *Nat. Struct. Mol. Biol. 11*, 918−926.
17. Walker, J. E., Saraste, M., Runswick, M. J., and Gay, N. J. (1982) Distantly related sequences in the alpha- and beta-subunits of ATP synthase, myosin, kinases and other ATP-requiring enzymes and a common nucleotide binding fold, *EMBO J. 1*, 945−951.
18. Hung, L. W., Wang, I. X., Nikaido, K., Liu, P. Q., Ames, G. F. L., and Kim, S. H. (1998) Crystal structure of the ATP-binding subunit of an ABC transporter, *Nature 396*, 703−707.
19. Smith, P. C., Karpowich, N., Millen, L., Moody, J. E., Rosen, J., Thomas, P. J., and Hunt, J. F. (2002) ATP binding to the motor domain from an ABC transporter drives formation of a nucleotide sandwich dimer, *Mol. Cell 10*, 139−149.
20. Chen, J., Lu, G., Lin, J., Davidson, A. L., and Quiocho, F. A. (2003) A tweezers-like motion of the ATP-binding cassette dimer in an ABC transport cycle, *Mol. Cell 12*, 651−661.
21. Diederichs, K., Diez, J., Greller, G., Mueller, C., Breed, J., Schnell, C., Vonrhein, C., Boos, W., and Welte, W. (2000) Crystal structure of MalK, the ATPase subunit of the trehalose/maltose ABC transporter of the archaeon *Thermococcus litoralis*, *EMBO J. 19*, 5951−5961.
22. Verdon, G., Albers, S. V., Dijkstra, B. W., Driessen, A. J., and Thunnissen, A. M. (2003) Crystal structures of the ATPase subunit of the glucose ABC transporter from *Sulfolobus solfataricus*: Nucleotide-free and nucleotide-bound conformations, *J. Mol. Biol. 330*, 343−358.
23. Hopfner, K. P., Karcher, A., Shin, D. S., Craig, L., Arthur, L. M., Carney, J. P., and Tainer, J. A. (2000) Structural biology of Rad50 ATPase: ATP-driven conformational control in DNA double-strand break repair and the ABC-ATPase superfamily, *Cell 101*, 789−800.
24. Zaitseva, J., Jenewein, S., Jumpertz, T., Holland, B., and Schmitt, L. (2005) H662 is the linchpin of ATP hydrolysis in the nucleotide-binding domain of the ABC transporter HlyB, *EMBO J. 24*, 1901−1910.
25. Benabdelhak, H., Schmitt, L., Horn, C., Jumel, K., Blight, M. A., and Holland, I. B. (2005) Positive co-operative activity and dimerization of the isolated ABC ATPase domain of HlyB from *Escherichia coli*, *Biochem. J. 386*, 489−495.
26. Guo, X., Harrison, R. W., and Tai, P. C. (2006) Nucleotide-dependent dimerization of the C-terminal domain of the ABC transporter CvaB in colicin V secretion, *J. Bacteriol. 188*, 2383−2391.
27. Koronakis, E., Hughes, C., Milisav, I., and Koronakis, V. (1995) Protein exporter function and in vitro ATPase activity are correlated in ABC-domain mutants of HlyB, *Mol. Microbiol. 16*, 87−96.
28. Holland, I. B., and Blight, M. A. (1996) in *Handbook of Biological Physics* (Konings, W. N., Kaback, H. R., and Lolkema, J. S., Eds.) Vol. 2, pp 111−135, Elsevier, Amsterdam.
29. Gaudet, R., and Wiley, D. C. (2001) Structure of the C-terminal ABC ATPase domain of human TAP1, the transporter associated with antigen processing, *EMBO J. 20*, 4964−4972.
30. Karpowich, N., Martsinkevich, O., Millen, L. L., Yuan, Y.-R., Dai, P. L., MacVey, K., Thomas, P. J., and Hunt, J. F. (2001) Crystal structures of the MJ1267 ATP-binding cassette reveal an induced-fit effect at the ATPase active site of an ABC transporter, *Structure 9*, 571−586.

31. Anderson, M. P., and Welsh, M. J. (1992) Regulation by ATP and ADP of CFTR chloride channels that contain mutant nucleotide-binding domains, *Science 257*, 1701−1704.
32. Zaitseva, J., Jenewein, S., Wiedenmann, A., Benabdelhak, H., Holland, I. B., and Schmitt, L. (2005) Functional characterization and ATP-induced dimerization of the isolated ABC-domain of the haemolysin B transporter, *Biochemistry 44*, 9680−9690.
33. Zhong, X., and Tai, P. C. (1998) When an ATPase is not an ATPase: At low temperatures the C-terminal domain of the ABC transporter CvaB is a GTPase, *J. Bacteriol. 180*, 1347−1353.
34. Hanahan, D. (1983) Studies on transformation of *Escherichia coli* with plasmids, *J. Mol. Biol. 166*, 557−580.
35. Studier, F. W., and Moffatt, B. A. (1986) Use of bacteriophage T7 RNA polymerase to direct selective high-level expression of cloned genes, *J. Mol. Biol. 189*, 113−130.
36. van Belkum, M. J., Worobo, R. W., and Stiles, M. E. (1997) Double-glycine-type leader peptides direct secretion of bacteriocins by ABC transporters: Colicin V secretion in *Lactococcus lactis*, *Mol. Microbiol. 23*, 1293−1301.
37. Sambrook, J., Fritsch, E. F., and Maniatis, T. (1989) *Molecular Cloning: A Laboratory Manual*, 2nd ed., Cold Spring Harbor Laboratory, Cold Spring Harbor, NY.
38. Harrison, R. W., Chatterjee, D., and Weber, I. T. (1995) Analysis of six protein structures predicted by comparative modeling techniques, *Proteins 23*, 463−471.
39. Harrison, R. W. (1999) A self-assembling neural network for modeling polymer structure, *J. Math. Chem. 26*, 125−137.
40. Horton, R. M. (1993) in *Methods in Molecular Biology* (White, B. A., Ed.) Vol. 15, Humana Press, Totowa, NJ.
41. Laemmli, U. K. (1970) Cleavage of structural proteins during the assembly of the head of bacteriophage T4, *Nature 227*, 680−685.
42. Gafni, J., and Ellerby, L. M. (2002) Calpain activation in Huntington's disease, *J. Neurosci. 22*, 4842−4849.
43. Yue, V. T., and Schimmel, P. R. (1977) Direct and specific photochemical cross-linking of adenosine 5′-triphosphate to an aminoacyl-tRNA synthetase, *Biochemistry 16*, 4678−4684.
44. Horn, C., Bremer, E., and Schmitt, L. (2003) Nucleotide dependent monomer/dimer equilibrium of OpuAA, the nucleotide-binding protein of the osmotically Regulated ABC transporter OpuA from *Bacillus subtilis*, *J. Mol. Biol. 334*, 403−419.
45. Zhao, Q., and Chang, X. B. (2004) Mutation of the aromatic amino acid interacting with adenine moiety of ATP to a polar residue alters the properties of multidrug resistance protein 1, *J. Biol. Chem. 279*, 48505−48512.
46. Yuan, Y., Blecker, S., Martsinkevich, O., Millen, L., Thomas, P. J., and Hunt, J. F. (2001) The crystal structure of the MJ0796 ATP-binding cassette: Implications for the structural consequences of ATP hydrolysis in the active site of an ABC-transporter, *J. Biol. Chem. 276*, 32313−32321.
47. Shyamala, V., Baichwal, V., Beall, E., and Ames, G. (1991) Structure-function analysis of the histidine permease and comparison with cystic fibrosis mutations, *J. Biol. Chem. 266*, 18714−18719.
48. Ambudkar, S. V., Kim, I. W., Xia, D., and Sauna, Z. E. (2006) The A-loop, a novel conserved aromatic acid subdomain upstream of the Walker A motif in ABC transporters, is critical for ATP binding, *FEBS Lett. 580*, 1049−1055.
49. Shyamala, V., Baichwal, V., Beall, E., and Ames, G. F. (1991) Structure-function analysis of the histidine permease and comparison with cystic fibrosis mutations, *J. Biol. Chem. 266*, 18714−18719.

BI061506I